In Situ Fabrication of Ribbed Wire Electrodes for Wire Electrochemical Micromachining

Zou Xianghe[1], Fang Xiaolong[1,2,], Zeng Yongbin[1,2], Zhang Pengfei[1], Zhu Di[1,2]*

[1] College of Mechanical and Electrical Engineering, Nanjing University of Aeronautics and Astronautics, Nanjing 210016, China
[2] Jiangsu Key Laboratory of Precision and Micro-Manufacturing Technology, Nanjing, 210016, China
[*] E-mail: xlfang@nuaa.edu.cn

Wire electrochemical micromachining (WECMM) is an electrochemical machining method in which a tensioned wire is used as the tool electrode. This paper proposes a novel method for in situ fabrication of ribbed wire electrodes. By applying high-speed rotation and reciprocating travelling to the ribbed wire electrode, the recycling of the electrolyte in the machining gap of WECMM was assumed to be accelerated, and this was helpful in the machining of high-aspect-ratio microstructures. Experiments were conducted to investigate the effects of pulse frequency, pulse duty cycle and electrolyte concentration on the ribbed groove size. Using optimized parameters, a ribbed wire electrode with a series of ribbed grooves, 113 μm in width and 100 μm in depth, was successfully fabricated. Finally, the feasibility of WECMM using a ribbed wire electrode was verified experimentally. A microstructure with wall widths of 230 μm and an aspect ratio of 87 was successfully fabricated from a stainless steel block 20 mm in thickness.

1. INTRODUCTION

Electrochemical machining (ECM) is a nontraditional machining process in which metallic material is removed by the mechanism of anodic dissolution in an electrolysis process [1]. As the tool electrode and the workpiece in ECM are not in contact during the machining process, no stress is transferred to the workpiece and there is no tool wear. Because of its advantages, ECM has been widely used in automotive, aerospace, electronics, optics, medical device and microsystem technologies [2-5].

Currently, ECM is an important method in the fabrication of microstructures with good surface integrity. Many high-aspect-ratio microstructures have been fabricated using electrochemical micromachining. Förster fabricated a micro-flow field structure for fuel cells in stainless steel [5]. Liu and Huang drilled micro-holes with a diameter of 400 μm in nickel-based alloys [6]. Much effort, such as on ultra-short pulses [7], tool vibration [8], tool insulation [9] and shaped tools [10], has been spent to enhance the aspect ratio and machining accuracy in electrochemical micromachining.

WECMM is an electrochemical micromachining method that uses a tensioned wire electrode as the cathode. The wire electrode cuts the workpiece for the fabrication of microstructures with a ruled surface. Because of these advantages, WECMM has become a promising method for fabricating high-aspect-ratio microstructures. Zhu et al. obtained some complex metallic micro-parts with structural dimensions of several micrometers [11]. Shin fabricated micro-features such as micro-grooves and gears in stainless steel plates [12]. However, as the thickness of the workpiece increases, the rapid removal of electrolysis products and renewal of the electrolyte from the narrow machining gap become difficult. Short circuits may frequently take place and destroy the stability of the machining process. It has been reported that using a method of axial electrolyte flow along the wire electrode [13], low frequency and small amplitude tool vibration [14], and reciprocating traveling wire [15] are helpful to improve the removal of the electrolysis products in the machining gap. Nonetheless, the route loss of electrolyte flow in a long and narrow machining gap is great and it limits the effect of flushing the electrolyte. The machining ability and efficiency of WECMM for a high-aspect-ratio microstructure are still inadequate for industrial applications.

A ribbed wire electrode that rotates at a high spindle speed and reciprocates in the axial direction could be helpful for refreshing the electrolyte. The ribbed groove structure will carry the dirty electrolyte in the machining gap out and bring fresh electrolyte into the machining gap. However, the preparation of a ribbed wire electrode is the premise. Yi and Zhang fabricated platinum probes with aspect ratios from 10 to 30 using two-step electrochemical etching [16]. Chiou et al. fabricated a tungsten micro-rod, 2 μm in diameter with an aspect ratio of 120, using ECM with an insulated iron needle cathode [17]. Liu et al. made several shaped micro-tools such as a semi-cylinder tool, thin slice tool and triangular prism [18]. Kuo and Huang fabricated a series-pattern micro-disk using micro-electrode discharge machining [19]. These methods are not suitable for the fabrication of a ribbed wire electrode with a large ratio of length to diameter (*L/D*).

This paper proposes a method for in situ fabrication of a ribbed wire electrode with large *L/D* ratio, which makes full use of the existing equipment and avoids the machining errors generated by holding the parts by fixture twice. The effects of pulsed voltage frequency, pulse duty cycle and electrolyte concentration on the ribbed groove size were investigated. Furthermore, the feasibility of WECMM using a ribbed wire electrode was experimentally investigated.

2. METHOD AND EXPERIMENTAL APPARATUS

As illustrated in Figure 1, a tensioned molybdenum wire was mounted in a small slot on the wire clamping apparatus. The wire electrode to be machined was immersed in the electrolyte and

rotated. With the feed motion of the molybdenum wire, a groove was electrochemically machined on the stainless steel wire electrode. Accordingly, a large *L/D* ratio ribbed wire electrode with a series of grooves was obtained.
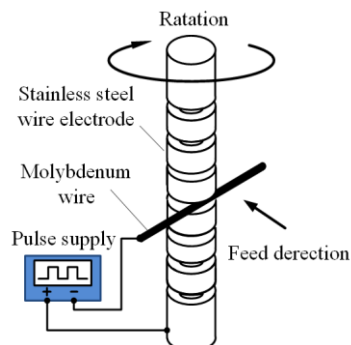
Figure 1. Schematic diagram of WECMM for preparing a ribbed wire electrode

Figure 2 illustrates the experimental apparatus for using WECMM for a ribbed wire electrode. The WECMM working system includes *X-Y* stages, a *Z* stage, a spindle, a fixture, a wire clamping apparatus, a pulse supply and an oscilloscope. The spindle is installed on the *Z*-axis, which will allow vertically reciprocating movement, and the feed motion is controlled by the *X-Y* stages. The fixture is used to ensure the rotation accuracy of the wire electrode because of its large *L/D* ratio.

In the experiments, a molybdenum wire 100 µm in diameter is used as the tool cathode, which is mounted on the clamping apparatus immersed in the electrolyte. The ribbed wire electrode, which is initially a stainless steel rod of 500 µm in diameter, functions as the anode.
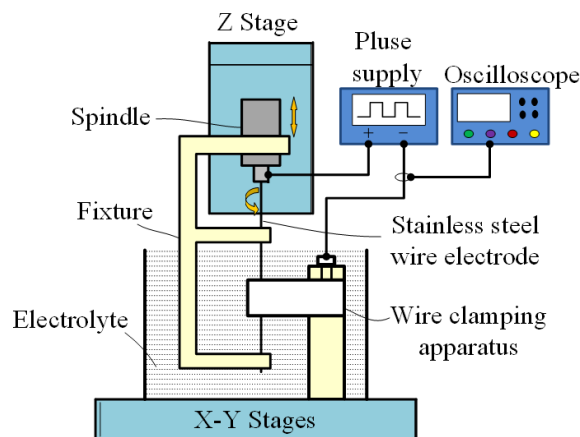
Figure 2. Experimental setup for WECMM

The machining conditions are listed in Table 1.

Table 1. Machining conditions

Parameters	Values
Applied voltage (V)	11
Pulse frequency (kHz)	1–100
Duty cycle (%)	10–30
Electrolyte solution	$NaNO_3$
Temperature (K)	298
Concentration (g/L)	15–35
Feed rate (μm /s)	0.1

The machining accuracy of the ribbed wire electrode was evaluated by the machined ribbed groove width. The widths of the grooves were measured using a digital microscope (DVM5000, Leica, Germany). Four measurements around a machined groove were taken for each sample in this study and the average width was obtained.

3. RESULTS AND DISCUSSION

3.1 Influence of pulse frequency on groove width

Figure 3 illustrates the influence of a pulse frequency from 1 to 100 kHz on the groove width at a duty cycle of 10% and an electrolyte concentration of 15 g/L. The groove width suffered a dramatic fall when the frequency increased from 1 to 10 kHz, and then it declined moderately as the frequency increased from 30 to 100 kHz. A narrow groove of width 112 μm was produced at a frequency of 100 kHz.

Figure 4 shows the groove structures fabricated at pulse frequencies from 1 to 100 kHz. With the increase of the pulse frequency, the edge blend of groove profile decreased and the side walls of the groove became more vertical. It showed that high frequencies massively elevated the feature resolution.
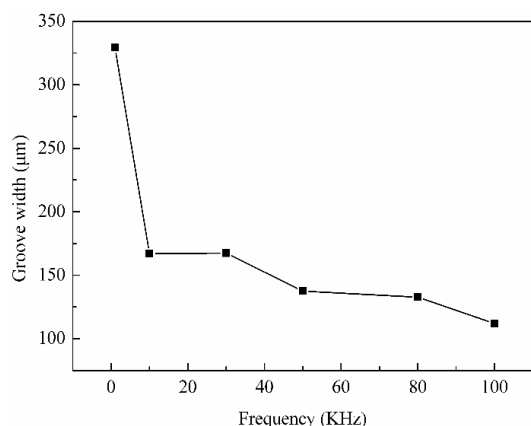
Figure 3. Variation of groove width with pulse frequency (applied voltage: 11 V, 10%; electrolyte: 15 g/L; spindle speed: 3000 rpm; and feed rate 0.1 μm/s)

In pulse ECM at high frequencies, the charge process of double layers cannot be ignored. Under certain conditions, the charge time is constant. As the pulse frequency increases, the effective machining time over a pulse period decreases. As a result, the material removal rate in a unit of time decreases. This explains that a high pulse frequency could narrow the side gap. This result is in agreement with the reports by Liu [20] and Koyano [21]. Liu reported the dissolution of a workpiece can be restricted to the region very close to the electrode using ultra-short pulses [20]. Koyano obtained significantly small side gap by applying ultra-short pulse ECM [21].

| (a) 1 kHz | (b) 10 kHz | (c) 30 kHz |
| (d) 50 kHz | (e) 80 kHz | (f) 100 kHz |
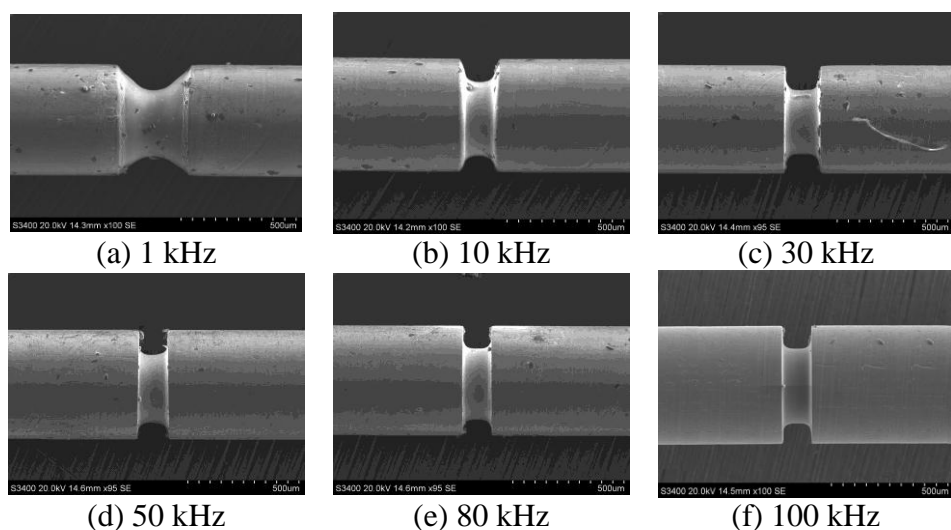
Figure 4. SEMs of grooves fabricated at different frequencies (applied voltage: 11 V, 10%; electrolyte: 15 g/L; spindle speed: 3000 rpm; and feed rate 0.1 μm/s)

3.2 Influence of pulse duty cycle on groove width
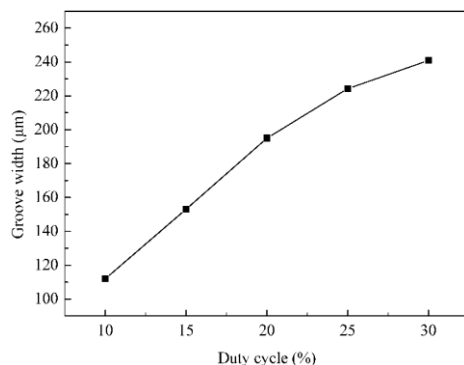
Figure 5. Variation of groove width with duty cycle (applied voltage: 11 V, 100 KHz; electrolyte: 15 g/L; spindle speed: 3000 rpm; and feed rate 0.1 μm/s)

Figure 5 illustrates the influence of the voltage pulse duty cycle on the groove width at a frequency of 100 kHz and an electrolyte concentration of 15 g/L. The groove width rose significantly from 112 to 274 μm as the duty cycle increased from 10% to 30%.

Figure 6 shows the groove structure fabricated as the pulse duty cycles from 10% to 30%. It showed that a high duty cycle lead to a taper generation of the side wall, and the size of the taper increased with the pulse duty cycle.

Obviously, a high pulse duty cycle leads to a long effective machining time. Therefore, a low duty cycle yielded a low material removal rate and a small side gap. Nonetheless, at a low duty cycle of below 10%, electrical short circuits usually occur because the material removal rate is too low, which makes the machining process unstable.

| (a) 10% | (b) 15% | (c) 20% |

| (d) 25% | (e) 30% |
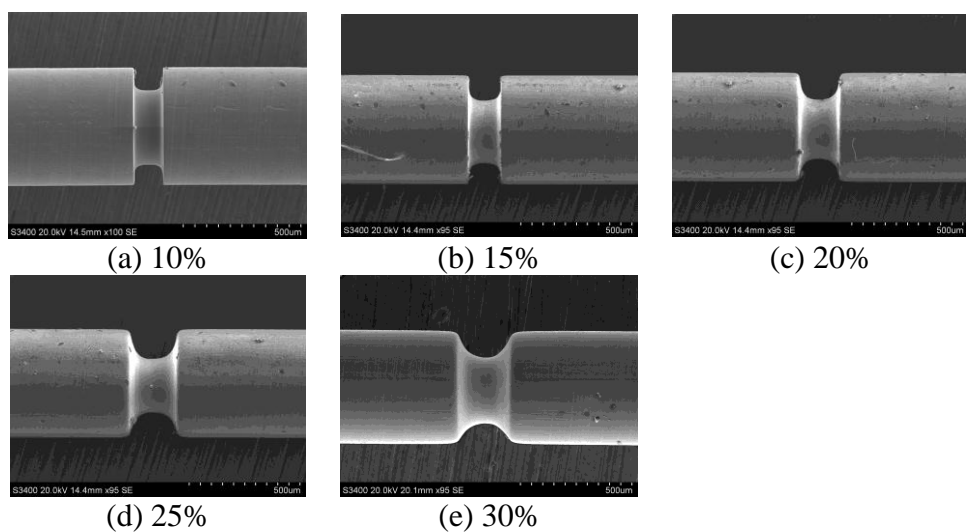
Figure 6. SEMs of grooves fabricated at different duty cycles (applied voltage: 11 V, 100 KHz; electrolyte: 15 g/L; spindle speed: 3000 rpm; and feed rate 0.1 μm/s)

3.3 Influence of electrolyte concentration on groove width

Figure 7 illustrates the influence of electrolyte concentration on the groove width at a frequency of 100 kHz and a duty cycle of 10%. As the concentration increased from 15 to 35 g/L, the groove width grew significantly.

Figure 8 shows the groove structure fabricated at concentrations from 15 to 35 g/L. It showed that high concentrations lead to a round angle generation at the bottom surface of the grooves, and the radius increased with the concentration.

It is clear that the current density is proportional to the electrolyte conductivity, which increases with the concentration. Hence, a high concentration leads to a large material removal rate and a groove with a large side gap. This result is agreed with the report by Sliva et al, which indicated that with low electrolyte concentration enabling higher accuracy than with high concentration in ECM process [22]. Nonetheless, at a low concentration of below 15 g/L, the cathode will come in contact with the

workpiece because the feed rate of the cathode exceeds the material removal rate. Otherwise, significant dissolution by the stray current occurs at high concentrations.
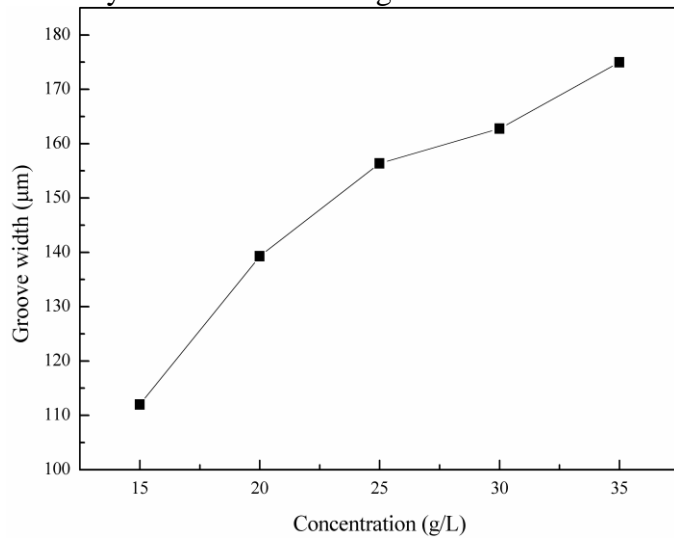
Figure 7. Variation of groove width with electrolyte concentration (applied voltage: 11 V, 10%, 100 KHz; spindle speed: 3000 rpm; and feed rate 0.1 μm/s)

(a) 15 g/L	(b) 20 g/L	(c) 25 g/L
(d) 30 g/L	(e) 35 g/L	
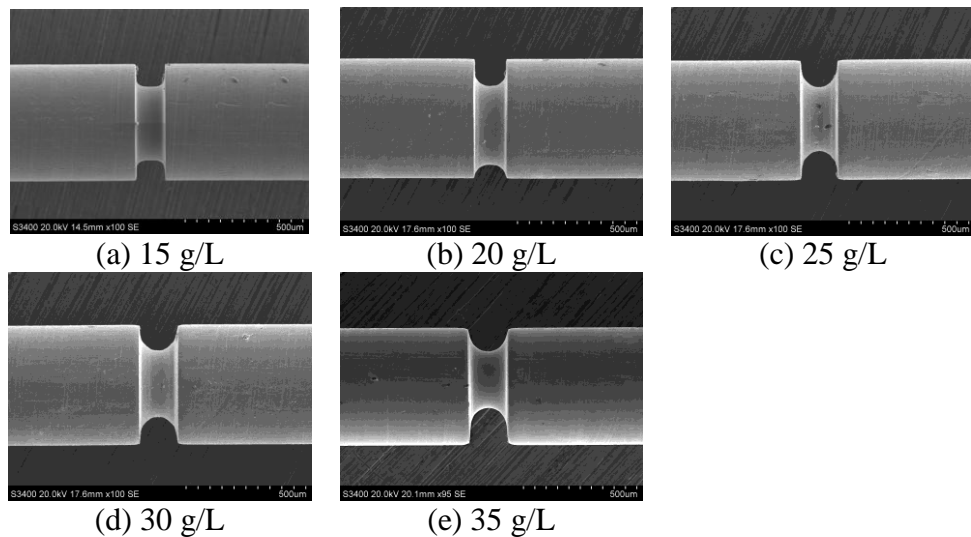
Figure 8. SEMs of grooves fabricated at different electrolyte concentrations (applied voltage: 11 V, 10%, 100 KHz; spindle speed: 3000 rpm; and feed rate 0.1 μm/s)

3.4 Fabrication of a large L/D ratio ribbed wire electrode

The above experiments indicate that the narrowest groove will be obtained at a pulse frequency of 100 kHz, a duty cycle of 10% and an electrolyte concentration of 15 g/L. A large *L/D* ratio ribbed wire electrode with a series of grooves was fabricated in stainless steel using the optimal parameters.

Figure 9 shows the fabricated structure, the averaged groove width and the averaged depth of which are about 113 μm and 100 μm, respectively.
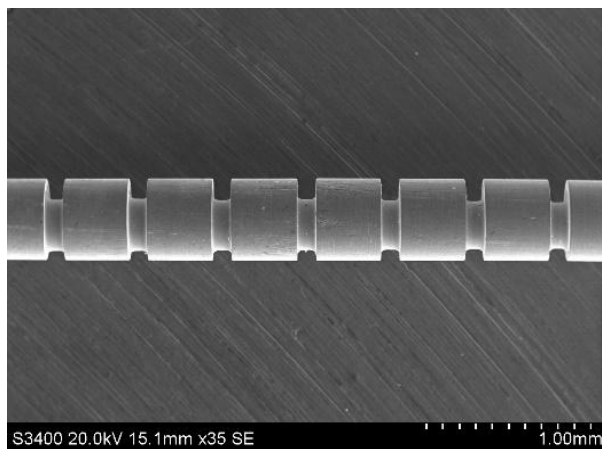
Figure 9. SEM image of ribbed wire electrode (applied voltage: 11 V, 10%, 100 KHz; electrolyte: 15 g/L; spindle speed: 3000 rpm; and feed rate 0.1 μm/s)

3.5. WECMM using a ribbed wire electrode

Figure 10 schematically depicts the principle of WECMM using a ribbed wire electrode. The workpiece immersed in the electrolyte acts as an anode, and a large *L/D* ratio ribbed wire electrode was used as the tool electrode. In the machining process, the ribbed wire electrode is rotated at high speed and it reciprocates in the axial direction. Under the combined action of the rotation and reciprocating motion, the electrolyte in the long and narrow machining gap is assumed to be renewed. This stirring of the electrolyte prevents the electrolysis products adhering on the surface of the ribbed wire electrode and the workpiece. When the ribbed wire electrode moves upward, it brings electrolysis products out from the machining gap to the top surface of the workpiece and carries fresh electrolyte into the machining gap from the bottom surface of the workpiece. When the electrode travels downward, it brings the products to the bottom and carries fresh electrolyte into the machining gap from the top surface.
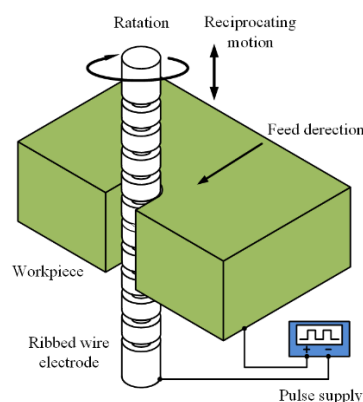
Figure 10. Schematic diagram of electrochemical micromachining with a ribbed wire electrode
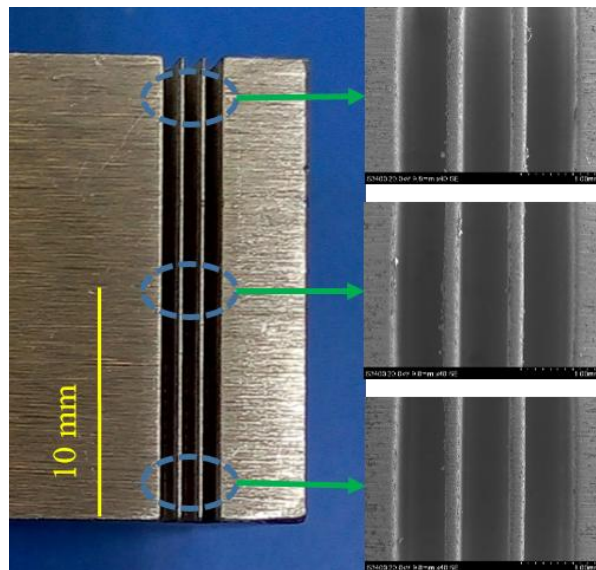
Figure 11. Machined high-aspect-ratio microstructure (applied voltage: 21 V, 40%, 100 KHz; electrolyte: 15 g/L; spindle speed: 5000 rpm; feed rate: 1 μm/s; reciprocating frequency: 1.5 Hz; and reciprocating amplitude: 20 mm)

A high-aspect-ratio microstructure in a stainless steel block 20 mm in thickness was fabricated using the machined ribbed wire electrode, as illustrated in Figure 10. The machining parameters were an applied voltage of 21 V, a pulse frequency of 100 kHz, a pulse duty cycle of 40%, a NaNO$_3$ electrolyte concentration of 15 g/L, an electrode feeding rate of 1 μm/s, a reciprocating frequency of 1.5 Hz, a reciprocating amplitude of 20 mm and a rotational rate of 5000 rpm. Figure 11 shows the fabricated microstructure, the average wall width of which is 230 μm and the aspect ratio is up to 87.

5. CONCLUSIONS

This paper proposed a method for in situ fabricating ribbed wire electrodes and its application for WECMM of high-aspect-ratio microstructures. Based on our experiments, these conclusions can be drawn:

(1)   The method is suitable for fabricating ribbed wire electrodes. A low pulse duty ratio and electrolyte concentration, and a high pulse frequency can confine the ribbed groove size.

(2)   Using optimized parameters, a ribbed wire electrode with a series of grooves of width 113 μm and depth 100 μm was successfully fabricated.

(3)   The feasibility of fabricating high-aspect-ratio microstructures using WECMM with a ribbed wire electrode was confirmed.

(4)   A structure with walls of width 230 μm and an aspect ratio of 87 was successfully fabricated in a stainless steel block of thickness 20 mm.

References

1. K.P. Rajurkar, D. Zhu, J.A. McGeough, J. Kozak and A. De Silva, *CIRP Annals - Manufacturing Technology,* 48 (1999) 567-579
2. K.P. Rajurkar, M.M. Sundaram and A.P. Malshe, *Proceedings of the Seventeenth Cirp Conference on Electro Physical and Chemical Machining (Isem),* 6 (2013) 13-26
3. M. Kock, V. Kirchner and R. Schuster, *Electrochimica Acta,* 48 (2003) 3213-3219
4. G. Li, D. Chen, J. Wang, C. Jian, W. He, Y. Fan and T. Deng, *Procedia Engineering,* 47 (2012) 362-365
5. R. Förster, A. Schoth and W. Menz, *Microsystem Technologies,* 11 (2005) 246-249
6. Y. Liu and S.F. Huang, *Advanced Materials Research,* 941 (2014) 1952-1955
7. S.H. Ahn, S.H. Ryu, D.K. Choi and C.N. Chu, *Precision Engineering-Journal of the International Societies for Precision Engineering and Nanotechnology,* 28 (2004) 129-134
8. B. Bhattacharyya, M. Malapati, J. Munda and A. Sarkar, *International Journal of Machine Tools and Manufacture,* 47 (2007) 335-342
9. B.J. Park, B.H. Kim and C.N. Chu, *CIRP Annals - Manufacturing Technology,* 55 (2006) 197-200
10. B.H. Kim, C.W. Na, Y.S. Lee, D.K. Choi and C.N. Chu, *CIRP Annals - Manufacturing Technology,* 54 (2005) 191-194
11. D. Zhu, K. Wang and N.S. Qu, *CIRP Annals - Manufacturing Technology,* 56 (2007) 241–244
12. H.S. Shin, B.H. Kim and C.N. Chu, *Journal of Micromechanics and Microengineering,* 18 (2008) 075009
13. S. Wang, Y. Zeng, Y. Liu and D. Zhu, *The International Journal of Advanced Manufacturing Technology,* 63 (2012) 25-32
14. S. Wang, D. Zhu, Y. Zeng and Y. Liu, *The International Journal of Advanced Manufacturing Technology,* 53 (2011) 535-544
15. N.S. Qu, H.J. Ji and Y.B. Zeng, *The International Journal of Advanced Manufacturing Technology,* 72 (2014) 677-683
16. Z. Yi and M. Zhang, *Review of scientific instruments,* 86 (2015) 085105
17. Y.C. Chiou, R.T. Lee, T.J. Chen and J.M. Chiou, *Precision Engineering,* 36 (2012) 193-202
18. Z. Liu, Y.B. Zeng and W.B. Zhang, *Advances in Mechanical Engineering,* 2014 (2014) 382105
19. C.L. Kuo and J.D. Huang, *International Journal of Machine Tools & Manufacture,* 44 (2004) 545-553
20. Y. Liu, D. Zhu, Y.B. Zeng, S.H. Huang and H.Y. Yu, *Chinese Journal of Aeronautics,* 23 (2010) 578-584
21. T. Koyano and M. Kunieda, *Procedia Cirp,* 6 (2013) 390-394
22. A.K.M.D. Silva, H.S.J. Altena and J.A. Mcgeough, *CIRP Annals - Manufacturing Technology*, 52 (2003) 165-168